# Nanomachining of (110)-oriented silicon by scanning probe lithography and anisotropic wet etching

F. S.-S. Chien, C.-L. Wu, Y.-C. Chou, T. T. Chen, S. Gwo, and W.-F. Hsieh

---

**Articles you may be interested in**

Single-electron transistor structures based on silicon-on-insulator silicon nanowire fabrication by scanning probe lithography and wet etching
J. Vac. Sci. Technol. B **20**, 2824 (2002); 10.1116/1.1523017

Silicon nanowires with sub 10 nm lateral dimensions: From atomic force microscope lithography based fabrication to electrical measurements
J. Vac. Sci. Technol. B **20**, 862 (2002); 10.1116/1.1470519

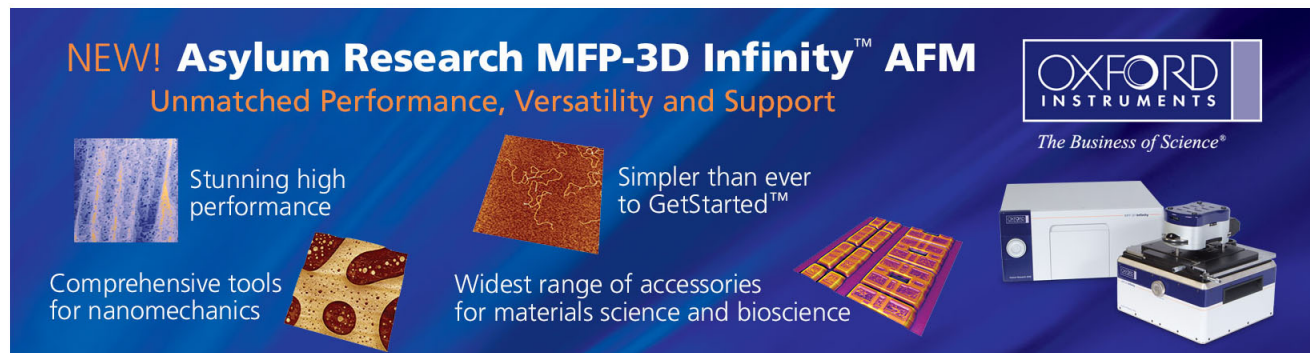Nano- and microchannel fabrication using column/void network deposited silicon
J. Vac. Sci. Technol. A **19**, 1229 (2001); 10.1116/1.1365129

Nano-oxidation of silicon nitride films with an atomic force microscope: Chemical mapping, kinetics, and applications
J. Appl. Phys. **89**, 2465 (2001); 10.1063/1.1339212

New approaches to atomic force microscope lithography on silicon
J. Vac. Sci. Technol. B **15**, 2912 (1997); 10.1116/1.589753

---

# Nanomachining of ⟨110⟩-oriented silicon by scanning probe lithography and anisotropic wet etching

F. S.-S. Chien,[a] C.-L. Wu, Y.-C. Chou, T. T. Chen, and S. Gwo[b]
*Department of Physics, National Tsing-Hua University, Hsinchu 300, Taiwan, Republic of China*

W.-F. Hsieh
*Institute of Electro-Optical Engineering, National Chiao-Tung University, Hsinchu 300, Taiwan, Republic of China*

We have demonstrated that silicon nanostructures with high aspect ratios, having ∼400 nm structural height and ∼55 nm lateral dimension, may be fabricated by scanning probe lithography and aqueous KOH orientation-dependent etching on the H-passivated (110) Si wafer. The high spatial resolution of fabricated features is achieved by using the atomic force microscope based nano-oxidation process in ambient. Due to the large (110)/(111) anisotropic ratio of etch rate and the large Si/SiO$_2$ etch selectivity at a relatively low etching temperature and an optimal KOH concentration, high-aspect-ratio gratings with (111)-oriented structural sidewalls as well as hexagonal etch pit structures determined by the terminal etch geometry can be obtained. © *1999 American Institute of Physics.* [S0003-6951(99)03242-8]

Micromachining, a microfabrication process for three-dimensional structuring, has emerged as one of the top priority research areas and may continue to be so in the coming years. In its extreme limit, nanomachining is aimed at the process of fabricating structures or devices with dimensions in the sub 100 nm regime. In the most widely used micromachining techniques borrowed from the microelectronic industry, lithography and subsequent pattern transfer are the key fabrication steps. In these techniques, patterns created by lithography in a resist, which determine the lateral resolution, must be transferred to the substrate by selective etching or deposition. Since high feature and large aspect ratios are required in the micromachining applications, a very faithful pattern transfer is necessary.

In the past, electron beam lithography or x-ray lithography has dominated the field of nanolithography. Recently, proximal probe induced anodic oxidation has become a promising scanning probe lithography (SPL) process that is capable of directly producing (without a resist) high-resolution (<100 nm) surface oxide patterns on a variety of materials. At present, atomic force microscope and scanning tunneling microscope (AFM/STM) based nano-oxidation of the (111) and (100) surfaces of H-passivated Si,[1–6] elemental metal,[2,7] and refractory metal nitride[8] films has been reported. Furthermore, several prototypes of micro devices have been demonstrated.[9,10] The nano-oxidation process is similar to the conventional electrochemical anodization except that an AFM/STM tip is used as the cathode and water from the ambient humidity is used as the electrolyte. Typically, a positive bias voltage (5–10 V) is applied to the sample with respect to the probe during nano-oxidation. The intense local electric field (initially, ∼10$^{10}$ V/m) desorbs the

H atoms and enhances the ionic transport of oxidant anions through the growing oxide layer. Therefore, by changing the experimental conditions such as scanning speed, sample bias, or ambient humidity, oxide patterns with controllable linewidths and heights/depths can be routinely achieved. So far, high-aspect-ratio pattern transfer of SPL produced oxides has been realized only with the (100)-oriented Si by Snow *et al.*[11] and Wilder *et al.*[12] using the dry etching techniques. However, Si wet bulk micromachining is the best-characterized micromachining tool and remains the most popular technique in industry. In the wet micromachining technique, (110)-oriented Si has been considered to be a more suitable material for high-packing-density and high-aspect-ratio applications.[13–15] In this letter we present a simple and reliable method for fabricating high-aspect-ratio (110)-oriented Si nanostructures by AFM-based nano-oxidation technology and wet etching.

Orientation-dependent etching (ODE) of crystalline Si has been known for a long time. Etching of (111) crystallographic planes is very slow compared with other planes. In the most used KOH/H$_2$O etchant system, a high anisotropic etch ratio of greater than 600:400:1 ({110}:{100}:{111}) can be routinely obtained.[14] Therefore, the etched microstructure geometry depends critically on surface mask pattern and alignment of (111) crystal planes with the surface. For (100)-oriented Si, the ODE process will proceed in the [100] direction into the substrate until the etch front hits the {111} planes, intersecting the (100) plane at the edge of the mask opening. The etch depth to oxide opening ratio is limited to 0.707:1, resulting in a low aspect ratio for the high-packing-density case. On the other hand, for the Si(110) case, four {111} planes are 90° to the (110) surface plane. This implies that we can etch vertical sidewalls with {111} side terminations. The extreme large anisotropic etch ratio between {110} and {111} indicates that very narrow lines, high aspect ratios, and very tight packing densities are possible with the (110) orientation technology.

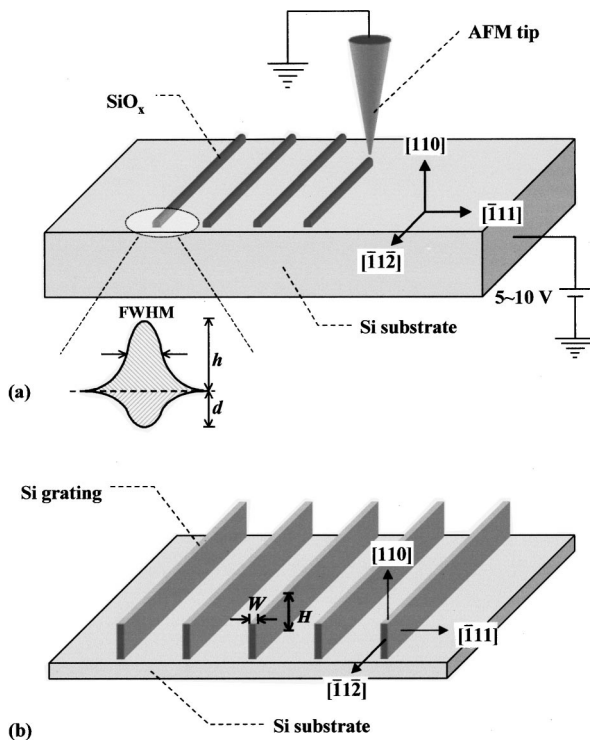In this work, silicon samples were cut from *n*-type (110)-

FIG. 1. Experimental procedure for fabricating gratings on (110)-oriented Si. (a) An oxide grating is patterned on the (110)-oriented Si by the AFM nano-oxidation process. The inset shows the cross section profile (both protruded and buried parts) of the oxide line. (b) A Si grating with ridge width $W$ and height $H$ appears after being transferred from the oxide grating using wet anisotropic etching.
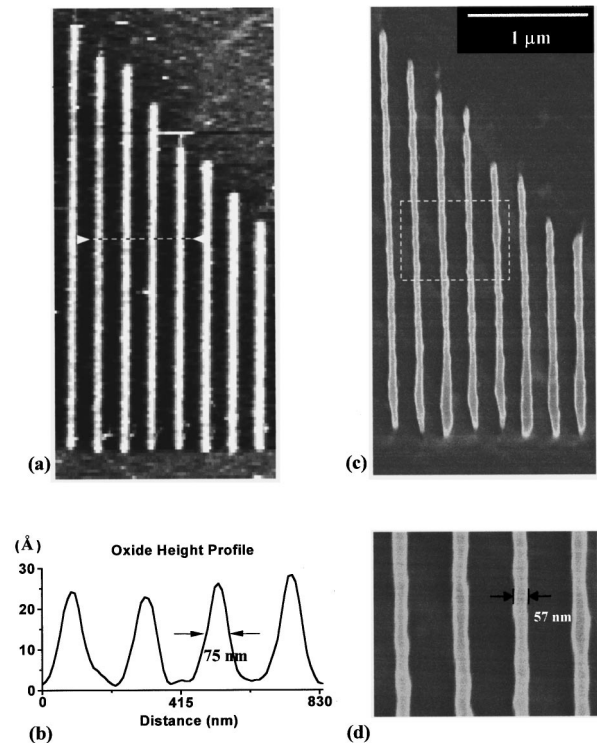


FIG. 2. (a) AFM image of a trapezoidal shape oxide grating patterned by AFM nano-oxidation. (b) AFM topographic height profile along the marked line in (a), showing the protruded height and FWHM of the oxide line. (c) SEM image of the Si grating after pattern transfer by etching in a KOH solution for 60 s. (d) Closeup SEM image of the marked area in (c).

oriented Si wafers with a resistivity of 5–6 $\Omega$ cm. The samples were passivated with hydrogen by dipping in a 1% aqueous HF solution for 20 s. The average surface roughness of the H-passivated films measured by AFM is $\sim 0.3$ nm. Local oxidation was performed in ambient using highly doped (0.01–0.025 $\Omega$ cm) Si cantilevers (10 nm average tip radius) and a commercial AFM/STM microscope (CP type, Park Scientific Instruments, CA). The average force constant and resonance frequency of the cantilevers used (Pointprobe®) are about 0.2 N/m and 13 kHz. The oxidation masks were formed by applying a sample bias of $+5-$ $+10$ V to the H-passivated Si(110) surfaces. Typical set point force and scanning speed are 1 nN and 1 $\mu$m/s, respectively. For patterning oxide gratings, the grating orientations with reference to the (110) wafer and the pattern transfer procedure are shown in Fig. 1. The cleaved {111} reference face facilitates the precise alignment of oxide lines along the $\langle 112 \rangle$ direction. The ODE etching was done with a 20 wt. % aqueous KOH solution at 50 °C. Under these conditions, the (110) silicon etch rate is $\sim 0.4$ $\mu$m/min and the thermally grown $SiO_2$ etch rate[16] is $\sim 0.33$ nm/min. After etching, the etch depths and structures were examined by means of a JEOL scanning electron microscope (SEM).

Shown in Fig. 2(a) is an example of oxide grating (pitch: 225 nm) obtained by AFM nano-oxidation at a sample bias of $+10$ V. The average full width at half maximum (FWHM) and the protruded oxide height $h$ displayed in the AFM topography profile analysis [Fig. 2(b)] are $\sim 75$ and $\sim 2.5$ nm, respectively. In order to estimate the ratio of volume expansion of AFM anodized oxide, previous studies

have compared AFM images of oxide patterns before and after selective HF etching. The volume expansion ratio determined by the protruded height $h$ and the buried depth $d$ of the oxide [$(h+d)/d$] was found to be around $3.0 \pm 0.4$ (2.27 for thermally grown oxide films).[2,4,6] Using this assumption, the total thickness $(h+d)$ of the oxide lines shown in Fig. 1 is $\sim 4$ nm. Figure 2(c) is a SEM micrograph of the same region after 60 s aqueous KOH etching. The grating depth is $\sim 400$ nm and the linewidth determined by SEM [Fig. 2(d)] is 55 nm, 27% narrower than the FWHM of the original AFM patterned oxide line. The reduction of linewidth after KOH etching is most likely due to the imperfect etch mask effect especially at the line edges, resulting from composition nonuniformity of the AFM-patterned oxides ($SiO_x$) induced by an inhomogeneous local electric field at the tip–sample junction.

The selectivity ratio between silicon and $SiO_2$ is very important for practical applications when a thin oxide is used as a mask during etching. This ratio depends strongly on the composition of the etchant and the etching temperature. For application using thin oxide masks, KOH solutions with a concentration of about 20 wt. % at a lower temperature ($\sim 50$ °C in our case) is preferable. The attainable ratio[16] is on the order of $> 1000$. The aspect ratio, defined as the structural height or depth to the minimum lateral dimension, is limited by the anisotropic ratio AR ($=R_{110}/R_{111}$) and selectivity $S$ ($=R_{110}/R_{SiO_2}$). If the effective lateral width of the oxide mask is $w_{ox}$ and the effective oxide height is $h_{ox}$, then the maximum achievable etching depth $H$ is determined by AR$\cdot w_{ox}/2$ or $S \cdot h_{ox}$. For the present case, the selectivity $S$ is larger than 1000 and the oxide height is $\sim 4$ nm. Therefore,
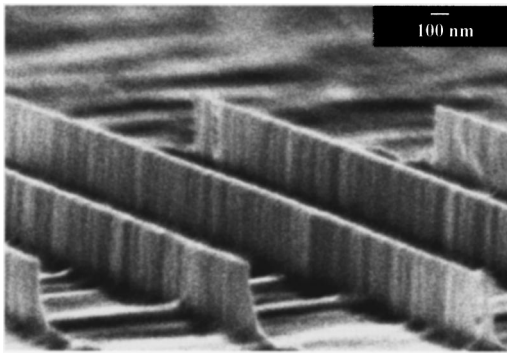
FIG. 3. SEM image of a high aspect ratio Si grating fabricated by AFM nano-oxidation and wet anisotropic etching in a KOH solution for 45 s. The vertical wall height is around 300 nm.
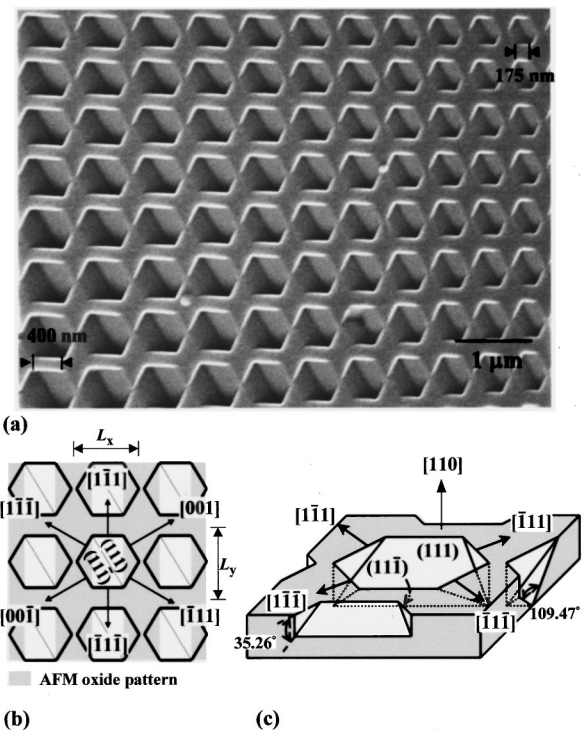


FIG. 4. (a) SEM image of a two-dimensional array of hexagonal pits with varied sizes on the (110)-oriented Si surface. (b) Illustration to indicate crystallographic directions of edges and bottom faces of hexagonal pits. The shadowed area is the oxide grid patterned by AFM nano-oxidation before pattern transfer. (c) Stereoscopic view of a hexagonal pit.

the ideal maximum structural depth is around 4 $\mu$m for the grating ridge. Figure 3 is a SEM micrograph of an etched grating with an etch depth of $\sim 300$ nm (45 s etching). The images of (111)-oriented sidewalls indicate that reasonably smooth (111)-oriented surfaces and excellent parallelism after etching can be obtained in this way. In practice, SPM oxide ($SiO_x$) is an imperfect etch mask because the structural and electrical properties of SPM oxide are inherently different from those of thermal oxide, which has a larger $S$ value.[2] Thus, there may be an intrinsic limitation to the etch depth that we can achieve.

Another useful approach to control the ODE process for fabricating Si nanostructures is the self-limiting process by the terminal etch geometry, which is determined by the orientations of the {111} planes with respect to the wafer surface. Figure 4(a) is a SEM image showing an example of obtainable structure. An array of etched hexagonal pits with varied dimensions, ranging from 175 to 400 nm, is made in this case. Figures 4(b) and 4(c) display the AFM oxide mask, a grid of vertically intersecting oxide lines with one of the axes along the $\langle 111 \rangle$ direction, for etching such a structure as well as a schematic of the etched hexagonal pit structure. The hexagons formed on the (110) surface is composed of the six traces of {111} planes intersected with the (110) plane. Inside each hexagonal pit, there are four vertical {111} sidewalls and two slant sidewalls with a characteristic 35.26° angle with respect to the (110) surface. Thus, the lateral pitches ($L_x$ and $L_y$) and linewidths of the AFM oxide grid can be used to precisely determine the etch pit sizes and depths. Once the hexagonal pit is completed during the ODE process, the etch rate of the {111} planes exposed is extremely slow and etching practically stops. Therefore, process sequences, which depend on achieving this type of well-defined final structure, are very uniform across the mask and very controllable.

In summary, AFM-based nano-oxidation is a viable technology for nanomachining the (110)-oriented Si. In contrast to the common belief, the KOH wet chemical method combined with the AFM-based nano-oxidation technology can etch structures reliably on the submicron scale. A low-cost and efficient method is presented here for fabricating both high-aspect-ratio gratings and hexagonal pit structures determined by the terminal etch geometry.

[1] J. A. Dagata, J. Schneir, H. H. Harary, C. J. Evans, M. T. Postek, and J. Bennet, Appl. Phys. Lett. **56**, 2001 (1990).

[2] J. A. Dagata, T. Inoue, J. Itoh, K. Matsumoto, and H. Yokoyama, J. Appl. Phys. **84**, 6891 (1998).

[3] E. S. Snow, P. M. Campbell, and P. J. McMarr, Appl. Phys. Lett. **63**, 749 (1993).

[4] Ph. Avouris, T. Hertel, and R. Martel, Appl. Phys. Lett. **71**, 285 (1997).

[5] R. García, M. Calleja, and F. Pérez-Murano, Appl. Phys. Lett. **72**, 2295 (1998).

[6] D. A. Fontaine, E. Dubois, and D. Stiévenard, J. Appl. Phys. **84**, 1776 (1998).

[7] H. Sugimura, T. Uchida, N. Kitamura, and H. Masuhara, J. Phys. Chem. **98**, 4352 (1994).

[8] S. Gwo, C.-L. Yeh, P.-F. Chen, Y.-C. Chou, T. T. Chen, T. S. Chao, S.-F. Hu, and T.-Y. Huang, Appl. Phys. Lett. **74**, 1090 (1999).

[9] S. C. Minne, H. T. Soh, Ph. Flueckiger, and C. F. Quate, Appl. Phys. Lett. **66**, 703 (1995).

[10] K. Matsumoto, M. Ishii, K. Segawa, and Y. Oka, Appl. Phys. Lett. **68**, 34 (1996).

[11] E. S. Snow, W. H. Juan, S. W. Pang, and P. M. Campbell, Appl. Phys. Lett. **66**, 1729 (1995).

[12] K. Wilder, C. F. Quate, D. Adderton, R. Bernstein, and V. Elings, Appl. Phys. Lett. **73**, 2527 (1998).

[13] D. L. Kendall, Appl. Phys. Lett. **26**, 195 (1975).

[14] K. E. Bean, IEEE Trans. Electron Devices **ED-25**, 1185 (1978).

[15] D. L. Kendall and G. R. de Guel, in *Micromachining and Micropackaging of Transducers*, edited by C. D. Fung, P. W. Cheung, W. H. Ko, and D. G. Fleming (Elsevier, Amsterdam, 1985), pp. 107–124.

[16] H. Seidel, L. Csepregi, A. Heuberger, and H. Baumgärtel, J. Electrochem. Soc. **137**, 3612 (1990).